

(21) Utilizing the National Corn-to-Ethanol Pilot Plant to Develop a Predictive Model for Distillers Dried Grain for the Fuel Ethanol and Animal Feed Industries

The objective of this two-year effort is to develop and validate a neural network predictive plant model for the composition of Distillers Dried Grain with Solubles (DDGS), a coproduct resulting from the dry grind fuel ethanol process.

Total project cost: \$807,221

Funding request: \$633,149

Project Lead: Southern Illinois University Edwardsville: National Corn-to Ethanol Research Center

Project Participants: Washington University, St. Louis, Missouri-Department of Chemical Engineering; Emerson Process Management; Illinois Department of Commerce and Economic Opportunity.

Start Date: May 23, 2005

End Date: May 23, 2007

Presentations/Publications

A publication based on Phase I trial data is in preparation.

A talk based on the results of this project was given on October 3, 2006 at the University of Missouri, Rolla Department of Chemical Engineering by James W. Taylor.

A presentation at the National Pork Board Meeting in November was given by John Caupert and included results from this grant.

Patents

None.

Progress in Past Quarter and Current Status

5.1.1. Experimental Design

In August, the NCERC performed a pilot-plant experiment to create a model of liquefaction and saccharification parameters to evaluate their effects on fermentation. The purpose of this experiment was to determine how changes in upstream processes affect the starting conditions of fermentation. The experimental design is shown in Table 1. Eleven operational factors were tested at two levels; eight of those factors were also tested at a third (midpoint) level. Plant operating conditions were changed every six hours. Samples of the mash were collected at two-hour intervals; so, three mash samples were collected for each experimental condition (a.k.a., “treatment” or “run”). The solids concentration and dextrose equivalent (DE) value were measured in every sample. One sample from every treatment was fermented in the lab to determine ethanol yield. The ethanol yield was estimated from the ethanol concentration after fermentation of the mash sample in the lab was complete.

5.1.2. Experimental Results

The main effects of each experimental factor shown in Table 1 were determined using standard statistical methods. Basically, the main effect of each factor is given by the difference between the average of the response variable (e.g., DE, ethanol yield) in all treatments in which the factor is present at its high level and all treatments in which the factor is present at its low level. In some experimental designs, interactions between factors can also

Table 1: Experimental conditions for evaluating the effects of upstream processing on fermentation*

Run	mill screen size (in)	process water flow (lbs/min)	target solids conc. (%)	slurry tank temp (°F)	slurry tank level (%)	slurry tank pH	slurry tank enzyme flow (g/hr)	jet cooker temp (°F)	mash tank temp (°F)	mash tank level (%)	mash tank enzyme flow (g/hr)
1	1/16	17.5	36	195	90	5.8	75	225	195	65	150
2	1/16	18.6	32	195	90	5.4	95	235	195	65	150
3	1/16	18.6	32	195	60	5.8	95	225	195	85	190
4	1/16	17.5	36	195	90	5.4	95	225	183	85	150
5	1/16	17.5	36	182	60	5.4	75	235	183	65	150
6	1/16	17.5	36	195	60	5.4	75	235	195	85	190
7	1/16	17.5	36	182	90	5.8	75	225	183	85	190
8	1/16	17.5	36	195	60	5.8	95	235	183	65	190
9	1/16	18.6	32	195	60	5.4	75	225	183	65	190
10	1/16	18.6	32	188.5	75	5.6	85	230	189	75	170
11	1/16	17.5	36	182	90	5.4	95	225	195	65	190
12	1/16	18.6	32	182	90	5.4	95	235	183	85	190
13	1/16	18.6	32	182	90	5.8	75	235	195	65	190
14	1/16	18.6	32	182	60	5.4	75	225	195	85	150
15	1/16	18.6	32	195	90	5.8	75	235	183	85	150
16	1/16	18.6	32	182	60	5.8	95	225	183	65	150
17	1/16	17.5	36	182	60	5.8	95	235	195	85	150
18	7/64	17.5	36	195	90	5.8	95	235	195	85	190
19	7/64	18.6	32	188.5	75	5.6	85	230	189	75	170
20	7/64	18.6	32	195	90	5.8	95	225	183	65	190
21	7/64	18.6	32	182	90	5.8	95	225	195	85	150
22	7/64	17.5	36	195	60	5.4	95	225	195	65	150
23	7/64	17.5	36	195	60	5.8	75	225	183	85	150
24	7/64	17.5	36	182	90	5.8	95	235	183	65	150
25	7/64	18.6	32	195	60	5.8	75	235	195	65	150
26	7/64	17.5	36	195	90	5.4	75	235	183	65	190
27	7/64	18.6	32	182	60	5.8	75	235	183	85	190
28	7/64	18.6	32	195	60	5.4	95	235	183	85	150
29	7/64	18.6	32	195	90	5.4	75	225	195	85	190
30	7/64	18.6	32	182	90	5.4	75	225	183	65	150
31	7/64	18.6	32	182	60	5.4	95	235	195	65	190
32	7/64	17.5	36	182	60	5.8	75	225	195	65	190
33	7/64	17.5	36	182	90	5.4	75	235	195	85	150
34	7/64	17.5	36	182	60	5.4	95	225	183	85	190

*the process water temperature was 200 °F and the jet cooker flow rate was 3 gal/min in all experiments

be evaluated, but the design used in this study involved too few treatments for the number of independent factors that were included. So, interactions could not be tested. Since treatments were not independently replicated, the statistical significance of the effects that were observed were evaluated by plotting the data in a way that allows detection of deviations from a normal distribution. The results of this analysis are shown in Figure 1 (DE) and Figure 2 (ethanol yield).

Normal-order plots are equivalent to plotting data on probability paper: data that are

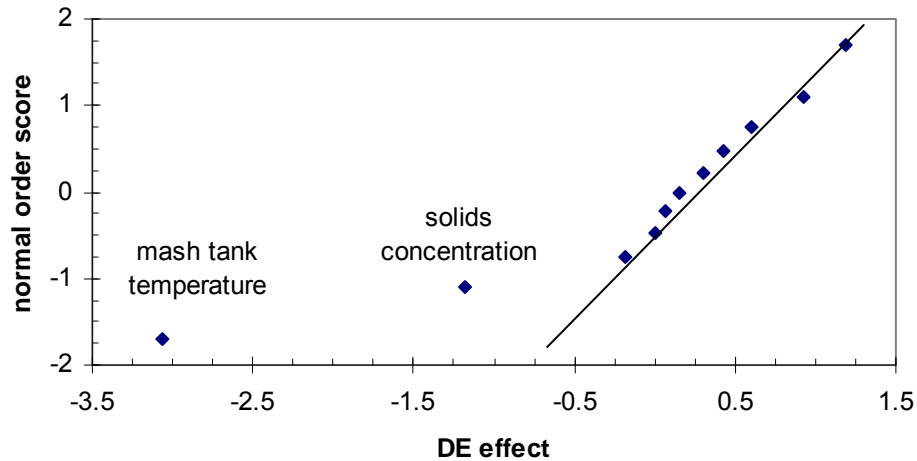


Figure 1: Normal-order plot of treatment main effects on mash DE. Effects that are statistically significant lie off of the straight line drawn through the remaining data points.

normally distributed plot approximately along a straight line with a slope that is proportional to the standard deviation of the distribution. Data that do not fall on the same straight line are likely to be drawn from different distributions. In Figures 1 and 2, statistically significant treatment effects can be identified by their location away from the straight line that is formed by the other data points. Figure 1 shows that the target solids concentration and the temperature of the mash tank both exerted statistically significant negative effects on the mash DE. That is, the DE was significantly lower when mash was prepared with the higher target solids concentration (36%) and at the higher mash tank temperature (195 °F).

Figure 2 shows that three factors exerted significant effects on ethanol yield: higher target solids concentrations and higher mash tank temperatures increased ethanol yield relative to the lower values for both factors (32% and

183 °F, respectively), and higher process water feed rate (18.6 lbs/min) reduced the ethanol yield relative to the lower feed rate (17.5 lbs/min). Note that process water feed rate and target solids concentrations are inversely proportional, such that the higher water feed rate always corresponds to the lower target solids concentration. So, it is not surprising that these two variables have different effects on ethanol yield. The fact that process water feed rate did not exert a significant effect on DE, whereas target solids concentration did, appears to reflect the nature of the distribution of treatment effects. As expected, the main effects of these two factors on DE were identical and of opposite sign (solids effect = -1.183 vs. process water feed rate effect = 1.183), but the process water feed rate effect was consistent with the distribution of the other treatment effects, whereas the solids concentration effect was not.

Because some treatment factors (e.g., slurry tank pH, mash solids concentration) could not be controlled well enough to insure that the actual level was equal to the target level,

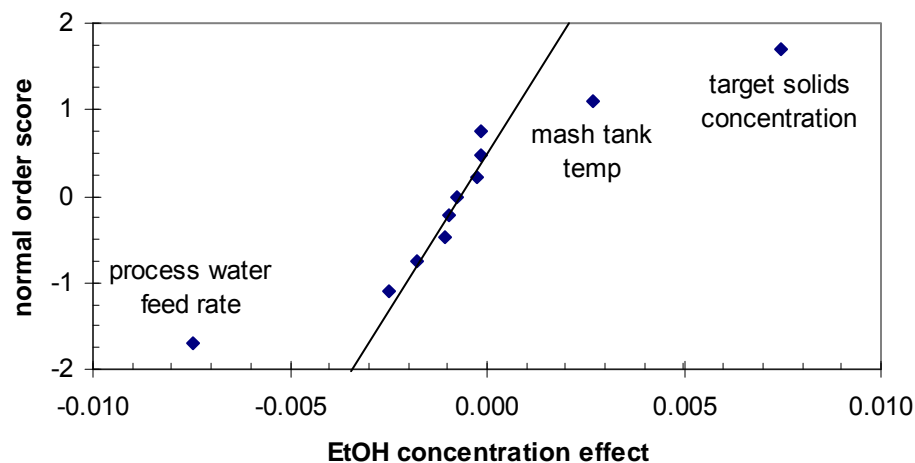


Figure 2: Normal-order plot of treatment main effects on the ethanol yield, measured as the ethanol concentration after lab-scale fermentation was complete. Note that treatment run 2 was excluded from this analysis because it was determined to be an outlier.

multiple linear regression was used to further evaluate the relationships between operational parameters and the performance variables of interest (i.e., mash DE and ethanol yield). This approach also allowed us to evaluate the effects of parameters that could be measured but which were not systematically varied and parameters that varied in response to the treatment conditions. For example, the effect of mash DE on ethanol yield can be included in a multiple linear regression model, but it cannot be considered in the factor analysis shown in Figs. 1 and 2. Multiple linear regression models have the following form:

$$\hat{y} = a_0 + a_1x_1 + a_2x_2 + \dots + a_ix_i + \dots + a_nx_n \quad (2)$$

where \hat{y} is the predicted value of the response variable of interest, x_i is the value of the “i”th independent variable, and a_i is the coefficient of the “i”th independent variable. The model coefficients, a_i , were estimated using the standard least squares approach.

The results of the multiple linear regression analysis are shown in Figs. 3 (mash DE) and 4 (ethanol yield). In these figures, the observed response variables are plotted versus the predicted response given by the best-fit model with the fewest independent variables. Only independent variables with coefficients that were significantly different from zero at the 95% confidence level were retained in the final model. The independent variables that were included in the final models (x_i), the best-fit model parameters (a_i), and the standard errors for each model parameter are shown in Table 2.

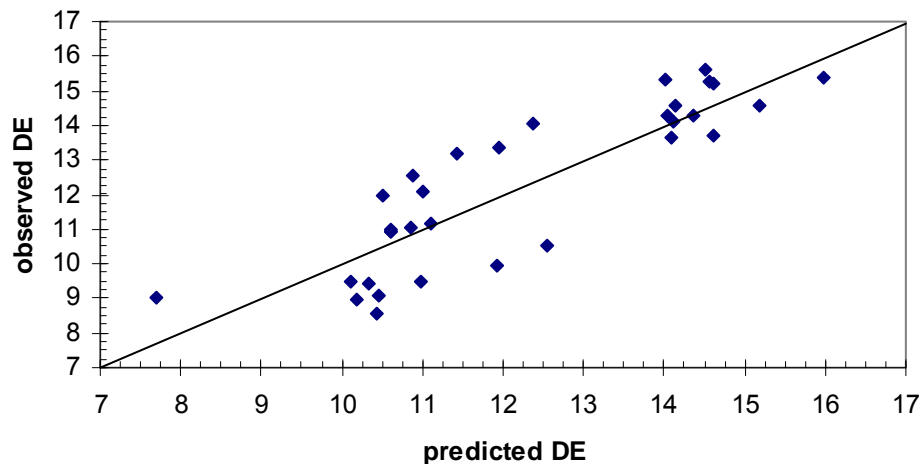


Figure 3: Best-fit multiple linear regression model for mash DE based on the operational parameters that were varied or measured in the mash-preparation experiment described in this report. The R^2 for this fit is 0.757, indicating that about three-quarters of the observed variation in mash DE is explained by the model. The measured mash solids concentration and the mash tank temperature were the only independent variables with model coefficients that were significantly different from zero. The diagonal line represents the expected relationship between observed and predicted mash DE if the model described the data perfectly.

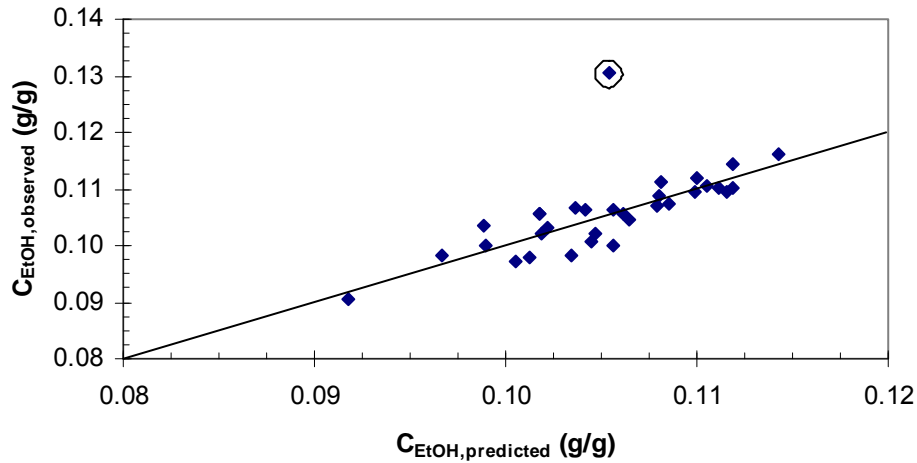


Figure 4: Best-fit multiple linear regression model for ethanol yield based on the operational parameters that were varied or measured in the STAC II pilot-plant study described in this report. The R^2 for this fit is 0.787, indicating that about three-quarters of the observed variation in ethanol yield is explained by the model. Process water feed rate, measured mash solids concentration, and mash DE were the only independent variables with coefficients that were significantly different from zero. The diagonal line represents the expected relationship between observed and predicted mash DE if the model described the data perfectly. The circled data point represents the observed ethanol yield for treatment run 2 (see Table 1 for experimental conditions), which was determined to be an outlier and, therefore, was not included in the regression analysis or the factor analysis.

Table 2: Best-fit parameters for multiple linear regression models for the effects of mash preparation conditions on mash DE and ethanol yield

response variable (y)	independent variable (x _i)	coefficient (a _i)	standard error
mash DE	intercept	82.04	7.41
	measured solids concentration (%)	-0.379	0.171
	mash tank temp (°F)	-0.303	0.04
ethanol yield (%)	intercept	11.8	2.91
	process water feed rate (lbs/min)	-0.383	0.103
	measured solids concentration (%)	0.194	0.047
	mash DE	-0.070	0.026

For both response variables, independent variables with model parameters that were significantly different from zero (Table 2) were also identified as exerting significant effects in the factor analysis (Figs. 1 and 2). The only difference is the mash tank temperature, which was important in the factor analysis for ethanol yield but not in the multiple linear regression. Since the mash tank temperature affected mash DE, and mash DE was included in the multiple-regression model, the positive effect of mash tank temperature on ethanol yield in the multiple-regression model might have been confounded by an opposing negative effect of mash DE.

5.1.3. Interpretation of Experimental Results

Mash tank temperature and mash solids concentration exerted negative effects on DE, which is a measure of the extent of starch hydrolysis. Higher DE indicates more hydrolysis and, consequently, smaller (on average) polysaccharide polymers. Therefore, the negative effect of these operational parameters on DE suggests that these factors inhibited starch hydrolysis. The effect of temperature may be explainable by the sensitivity of the amylase enzyme that is added to the mash tank along with the corn-flour slurry. The rate of enzyme-catalyzed reactions typically increases with increasing temperature until the maximum temperature is reached, after which the rate decreases rapidly with further increase in temperature. The maximum temperature of the enzyme appears to be closer to the low end of the temperature range used in this experiment (183 °F) than the high end (195 °F). The best-fit coefficient for mash tank temperature in the multiple regression model suggests that the DE should decrease by about 4 units in going from the lowest to the highest temperature. The actual range of observed DE values was about 7 units, suggesting that the temperature effect could explain about half of the observed variation. The temperature optimum of the enzyme used in this study might be available from the vendor. This information should be obtained and compared to these results.

The effect of mash solids concentration may have a more mundane explanation: since DE is a ratio, if the change in solids concentration increases the total starch concentration more than it increases the reaction rate, DE will decrease. The dextrose equivalent (DE) value is basically a measure of the number of reducing sugar units relative to the total number of sugar monomers in the starch polymer. The change in the starch concentration—and therefore, the total number of sugar monomers in the polymer—is linearly proportional to the change in the solids concentration, but the rate of enzyme catalyzed reactions is not a linear function of substrate concentration. Instead, the reaction rate, r , can be described by a function similar to the Michaelis-Menten equation:

$$r = \frac{V_{\max}S}{K_m + S} \quad (3)$$

where V_{\max} is the maximum rate of the reaction, which occurs when the enzyme is saturated with substrate, S is the substrate (starch in this case) concentration, and K_m is the half-saturation concentration (i.e., the substrate concentration at which the reaction rate is half maximal). Equation (3) shows that the reaction rate is linearly proportional to the substrate concentration only at substrate concentrations that are very low relative to

K_m . Assuming that corn flour is about 70% starch by mass, the starch concentration at the lowest target solids concentration will be about 22% (220 g/L), which is probably high relative to the K_m . So, any increase in the starch concentration that occurs in response to increasing solids concentration is unlikely to be matched by a proportional increase in the reaction rate; in fact, it is more likely that the reaction rate will change very little. Therefore, the DE will decrease because the denominator of the ratio will increase faster than the numerator. The best-fit coefficient for the effect of solids concentration on mash DE (Table 2) suggests that the DE should decrease by about 1.5 units over the range of values that were tested in this experiment. Therefore, the effect of solids concentration on DE is smaller than the effect of temperature.

The two factors with the biggest effect on ethanol yield are highly correlated: mash solids concentration and process water feed rate. Increasing the process water feed rate at a constant rate of corn feed to the hammermill will result in a proportional decrease in the solids concentration of the slurry, which will be reflected in the solids concentration of the mash. Therefore, it is not surprising that these two operational parameters have opposite effects on ethanol yield. Dextrose equivalent also affects ethanol yield, but the magnitude of the effect is relatively small (i.e., the observed range in DE can account for less than one-fifth of the observed range of final ethanol concentrations) and opposite to the expected direction (i.e., higher mash DE produced lower final ethanol concentrations). The effects of solids concentration and process water feed rate, on the other hand, can account for about two-thirds of the observed variation, and the effect is in the expected direction. The importance of mash solids concentration on ethanol yield is not surprising because the fermentation was allowed to go to completion, and a higher initial substrate (starch) concentration would be expected to produce a higher final product (ethanol) concentration. The relatively small role of DE probably also reflects the fact that this was an endpoint measurement. The effect of DE might have been greater (and positive) if ethanol production kinetics had been measured instead of the final ethanol yield.

5.2 Neural Network Model for Mash Dextrose Equivalent (DE)

The results of a neural network model of the DE number with respect to plant process parameters are shown in Figures 5 and 6, which show plots of the predicted mash DE versus measured DE during the STAC II trial. Figure 6 uses a different and more rigorous method of cross-validation, called random hold-back. The R^2 value for neural nets is much greater than for traditional regression, and both analysis methods exhibit good predictive power. This shows that neural nets with high correlation between the DE number and the plant process parameters can be produced. Unfortunately, these models do not provide an estimate of the effect of a single process variable. Instead, they provide predictions based on the overall state of the process.

5.3 Phase III Pilot-Plant Study: Effect of Process Conditions on DDGS

In October, a plant trial was undertaken to create DDGS at different conditions in both the slurry and drying systems. Over 60 DDGS samples were collected at the different

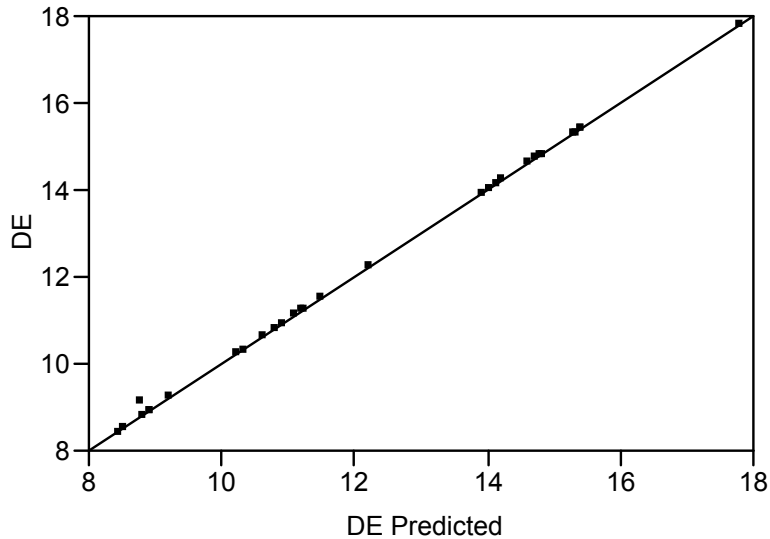


Figure 5: Neural network model predicted mash DE versus observed DE using K-fold cross-validation

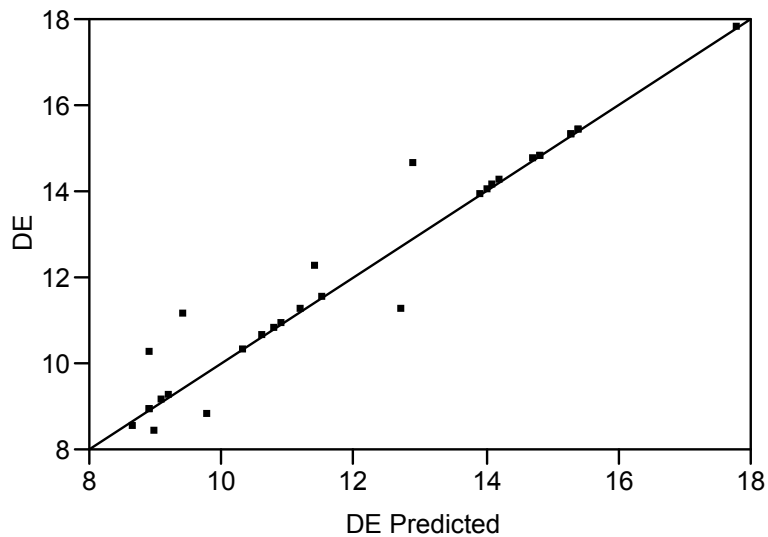


Figure 6: Neural network model predicted mash DE versus observed DE using random holdback (66% training, 33% testing) fitting procedure

conditions. Nine fermentations remain to obtain the remaining DDGS samples to create a

comprehensive data set for analysis. The final trial of this grant is scheduled to be completed in January.

6. Plans for the following quarters

Preparations are being made to complete the final pilot-plant experiment sponsored by this grant. This experiment and the one completed in October are investigations of factors that were identified as exerting significant effects in previous plant trials. The impact of these factors on DDGS nutritional values will be measured. The pilot-plant study conducted in October used a hammermill screen size of 1/16 inch, and the study that will be conducted in January will use a screen size of 7/64 inch. Upon the completion of the final pilot-plant experiment, DDGS samples will be analyzed and the data from all of the studies will be compiled. The remaining time in the grant will focus on disseminating the results from these trials to the academic and industrial communities.

7. References

1. Tilstra, H. (2005) in *Distillers Grains Quarterly* pp 25-26.
2. Thaler, B. (2002) Use of Distillers Dried Grains with Solubles (DDGS) in Swine Diets. *Extension Extra*.
3. Belyea, R. L., Rausch, K. D., and Tumbleson, M. E. (2004) Composition of corn and distillers dried grains with solubles from dry grind ethanol processing. *Bioresour Technol* 94, 293-8.
4. Blevins, T. L., McMillan, G. K., Wojsznis, W. K., and Brown, M. W. (2002) *Advanced Control Unleashed*, ISA Press, Research Triangle Park, NC.
5. Stein, H. H., Gibson, M. L., Pedersen, C., and Boersma, M. G. (2006) Amino acid and energy digestibility in ten samples of distillers dried grain with solubles fed to growing pigs. *J Anim Sci* 84, 853-60.
6. Cromwell, G. L., Herkelman, K. L., and Stahly, T. S. (1993) Physical, chemical, and nutritional characteristics of distillers dried grains with solubles for chicks and pigs. *J Anim Sci* 71, 679-86.
7. Rosentrater, K. (2005) in *Distillers Grains Quarterly* pp 15-17.
8. Latta, M., and Eskin, M. (1980) A Simple And Rapid Colorimetric Method For Phytate Determination. *Journal Of Agricultural And Food Chemistry* 28, 1313-1315.

8. Appendix

What does Dextrose Equivalent Mean?

The dextrose equivalent or DE test is widely used as a measure of the extent of conversion of starch to glucose. Chemically, the DE test determines the number of glycosidic bonds that have been broken relative to an initial number of intact glycosidic bonds.

$$DE = 100 \times \left(\frac{\text{Number of reducing ends}}{\text{Number of } \alpha-1,4 \text{ bonds}} \right)$$

To give an example, let's take a single 1000 glucose long polymer of starch. To simplify matters, we will assume it is amylose, which contains no branches. If we put that starch molecule in solution there are two ends to the chain, but only one of those can react chemically and is called the **reducing end**. Now let's add some α -amylase for a few moments and break that 1000 unit starch into 100 ten unit pieces. Now there are 100 exposed reducing ends of the polymer out of an initial number of 999 unexposed ends. This would correspond to a DE number of $100 \times (100/999) \approx 10$.

Since the DE test determines the fraction of available ends, it is closely related to the degree of polymerization (DP) of starch. To a good approximation,

$$DP = \frac{100}{DE}$$

Thus, in our previous example, the average size of the starch polymer chains is $100/10 = 10$ units of glucose. Now, in the real world not all starch chains are the same length. A distribution of chain lengths exists. However, DP is still the number average length of the chains as defined by a number weighted average.

$$DP = \frac{\sum_i n_i X_i}{\sum_i n_i}$$

The chain length of each type of starch chain, i , is X_i and the number of those chains have that molecular weight is n_i .

Thus, ultimately the DE test gives us the average length of the starch polymers in solution, but it does not give us an idea of the distribution of these molecules. For example, take a solution containing a 1000 unit starch molecule and break it into 25 chains of 20 glucose units each and 100 chains of 5 glucose units each. The DE test would find 125 reducing ends out of 999 for a value of 12.5. The predicted chain length

would be $100/12.5 = 8$ units, but there are no eight unit starches in solution, only a mixture of 5 and 20 units.

To get an idea of the dispersion of the starch chains around the mean, one needs the polydispersity, P . Polydispersity is the ratio of a weighted average of molecular weight to a number average of molecular weight.

$$\bar{M}_n = \frac{\sum_i n_i M_i}{\sum_i n_i}$$

$$\bar{M}_w = \frac{\sum_i n_i M_i^2}{\sum_i n_i M_i}$$

$$P = \frac{\bar{M}_w}{\bar{M}_n}$$

Polydispersity is measure of the distribution of molecular weights of the polymer, similar to standard deviation in principle. Polydispersity can be determined using an HPLC column that can measure the distribution of sugar molecules sizes with a size exclusion column. With both the average chain length or average chain molecular weight and the polydispersity a suspension of small-chained starch molecules can be characterized using normal statistics.

DE is perhaps the most important initial parameter in fermentation and determines the extent of both sugar and alcohol production in fermentation. In addition, it can determine the extent to which the yeast metabolism occurs and changes the chemical composition of fermentation.

Plans for the next quarter

(22) Iron-Based Mixed Metal Carbide Fischer-Tropsch Catalysts

This three-year effort will seek to develop a more active, selective, attrition resistant and stable Fe FTS catalysts based on formulations containing a second metal (besides Cu) capable of forming mixed metal carbides with Fe.

Total project cost: \$1,334,594

Funding request: \$875,499

Project Lead: Clemson University

Project Participants: Louisiana State University; RTI; Rentech; Sud-Chemie, Inc.; South Carolina Energy Office; Louisiana State Energy Office

Start Date: August 31, 2005

End Date: August 31, 2008

Presentations/Publications

None.

Patents

None.

Progress in Past Quarter and Current Status:

Project activities are progressing in accordance with the project schedule (Table 1). During this third quarter of activities the main focus has been on catalyst preparation characterization, and reaction studies. These activities are described in the following section comprising the experimental methodology and results.

2.1 Methodology

2.1.1 Catalyst Preparation

Catalysts are being prepared according to the general formulation: $100-x)Fe/xMe/5Cu/17Si$, where *Me* indicates a second-metal, and *x* is the atom% and is 10 or smaller. During this quarter, we have prepared Fe-based catalysts with 3, 5, 7 and 10 atom% of Cr and Zr using the constant pH precipitation technique [1, 2]. Catalyst preparations make use of three solutions containing catalyst precursors at the desired molar ratio of components; $Fe(NO_3)_3 \cdot 9H_2O$ (~0.6 M), $Cu(NO_3)_2 \cdot 3H_2O$ and tetraethylorthosilicate ($Si(OC_2H_5)_4$, TEOS). The first 2 solutions are dissolved in 60 ml of water where the latter is dissolved in 40 ml of propanol in order to obtain total volume of 100 ml. Second metal precursors used are Cr(III) NO_3 and Zr(IV) $(NO_3)_2 \cdot xH_2O$ for which its concentration depends on the desired Fe/*Me* molar ratio. Then the solutions are mixed first in a stirred round-bottom flask at $83 \pm 3^\circ C$. Once the temperature reaches $83^\circ C$, aqueous NH_3 (□2.7 M) also at $83 \pm 3^\circ C$ is slowly added under vigorous and continuing stirring for 3 min. The resulting pH after formation of a precipitated is 8-9. The precipitate is aged in a vessel at room temperature for 17-18 h then thoroughly washed with deionized water to remove excess NH_3 until pH is 7-8 (1.3-1.5 liters of deionized water used). The washed precipitate is dried in an oven for 18-24 h at $120^\circ C$ to remove excess water. After drying, the catalyst precursor is calcined in static air at $300^\circ C$ for 5 h, then cooled to room temperature over a 2-h period in a muffle furnace. A fresh calcined catalyst is sieved $< 90 \mu m$ before reaction testing and other characterizations.

2.1.2 Catalyst Characterization

Catalysts are characterized by elemental analysis, N_2 adsorption (BET, pore volume, pore size distribution), XRD (Fe and *Me* crystalline phases formed), and CO pulse chemisorption (surface metal atoms).

a) Elemental Analysis

Elemental analysis is performed to determine the composition of elements in the bulk of catalysts. The composition content of catalysts is determined using ICP-OES at Galbraith Laboratories.

b) N_2 Adsorption

The BET surface area, pore volume, average pore diameter, and pore size distribution of the catalysts are determined by N_2 physisorption using a Micromeritics ASAP 2010 automated system. A 0.3 g catalyst sample is degassed in the Micromeritics ASAP 2010 at $100^\circ C$ for 1 h

and then at 300°C for 2 h with 10°C/min ramping rate prior to analysis. The analysis is done using N₂ adsorption at -196 °C.

c) X-Ray Diffraction (XRD)

XRD is used to determine the phase composition of Fe catalysts as prepared and after pretreatments. The XRD spectrum of the catalysts is collected using an X-ray diffractometer, Scintag 2000 x-ray diffractometer, using monochromatized Cu K_α radiation (40 kV, 40 mA) and a Ge detector using a step scan mode at a scan rate of 0.02° (2θ) per second from 10-80°. XRD peak identification is done by comparison to the JCPDS database software.

d) CO-Pulse Chemisorption

Fe dispersion is determined by pulsing CO over the reduced catalyst. Approximately 0.2 g of catalyst is put in a quartz tube, incorporated in a temperature-controlled oven and connected to a thermal conductivity detector (TCD). He is used as a carrier gas for this system. Prior to chemisorption, the catalyst is reduced in a flow of hydrogen (50 cc/min) at 280°C for 12 h.

Afterwards, the sample is cooled down to 35 °C with He 30cc/min. CO is pulsed at 35°C over the reduced catalyst until the TCD signal is constant. An assumed stoichiometry ratio on the surface of CO:Fe_s = 1:2 is used [3].

e) Extended X-ray absorption fine structure (EXAFS)

EXAFS is used to provide information on the structure and coordination of atoms on the catalyst surface. The catalysts are studied at the Center for Advanced Microstructures and Devices (CAMD) at LSU.

2.1.3 CO Hydrogenation Reaction Studies

CO hydrogenation is performed using 0.1 g of catalyst packed in a fixed bed-quartz reactor with i.d. = 8 mm. The total flow rate used is 60 cc/min with the H₂/CO ratio of 2/1 in a balance of He. The catalyst sample is pretreated in 30 cc/min of H₂ at 280 °C for 12 h with 2 °C/min ramping rate prior to CO hydrogenation.

CO hydrogenation reactions are carried out at 280 °C and at 1.8 atm. The product streams are analyzed by gas chromatography.

2.2 Results and Discussion

During this quarter, we have done some characterization of the catalysts with 5 atom% of added metal prepared in the 4th quarter of the project (3rd quarter 2006). N₂ adsorption, elemental analysis and H₂ TPR were employed for determining the BET surface area, the metal content and the reduction of metal, respectively. The BET surface area results are shown in Table 2 where the element content and TPR peak results are shown in Table 3 and Fig. 1, respectively.

It appears that the BET surface area of the catalyst did not significantly correspond to the observed activity. The surface area was ranged from 295-373 m²/g. However, the lowest catalyst activity observed for the FeW catalyst appears to be a result of having the lowest BET surface area. Similarly, adding transition metal did not have significant impact on the reduction of Fe. The TPR peaks appear to be similar for all catalysts with a small difference in peak temperature and degree of reduction. Precise %reducibility of Fe will be calculated in the future.

Table 2: The BET surface area, pore volume and pore size of Fe-based catalysts.

Catalyst ^a	Max Rate ^b	BET S.A.	Pore volume	Pore size (A)
-----------------------	-----------------------	----------	-------------	---------------

	($\mu\text{mol/g/s}$)	(m^2/g)	(cm^3/g)	
95Fe/5Zr	2.94	350	0.29	33
95Fe/5Cr	1.98	351	0.29	33
95Fe/5Mn	1.51	373	0.32	34
95Fe/5V	1.26	338	0.26	30
95Fe/5Ta	1.09	341	0.29	34
95Fe/5Mo	1.10	342	0.27	32
95Fe/5W	0.48	295	0.25	34
100Fe	0.74	329	0.34	42

^a with 5Cu/17SiO₂

^b total rate of hydrocarbon and CO₂ production

Table 3: The elemental content and peak temperature for TPR.

Catalyst ^a	Element Content (atom%)			TPR peak temperature (°C)
	Fe	Me		
95Fe/5Zr	-	-	-	285
95Fe/5Cr	88.2	4.6	4.5	289
95Fe/5Mn	80.5	4.0	3.3	288
95Fe/5V	-	-	-	325
95Fe/5Ta	-	-	-	295
95Fe/5Mo	-	-	-	292
95Fe/5W ^b	80.8	4.2	4.1	310
100Fe	93.9	0.0	3.9	300

^a with 5Cu/17SiO₂

^b contains 60 ppm of Cl residue

The catalysts were also characterized by EXAFS determining the K-edge for Cu spectra. Table 4 below shows the samples for testing. XANES and EXAFS for the Fe were taken both in transmission and electron yield for all samples except those denoted by an asterisk. Cu electron yield and transmission data were taken on most samples, but information from the data will be difficult, if not impossible to extract because the data is extremely noisy (the metal loading is at the detection limit for electron yield and transmission). Mo, Cr, and W data were taken on the samples that contained these metals. The Fe XANES data will be difficult to interpret until a standard for Fe C_x is synthesized using techniques described in the literature [5-8]. The iron carbide will be synthesized first in an Altamira AMI-200R-HP at LSU then within the Lytle cell at CAMD. The Fe EXAFS data can be interpreted once XRD data is taken to give the phases that are in the sample (at LSU/CAMD). Data from Clemson suggest that Zr causes the highest activity for the Fischer-Tropsch synthesis, therefore it will be desirable to study a passivated Zr sample

Catalyst tested in parts by weight (synthesized in Clemson University laboratories): 100 Fe / 5 Cu / 17 Si (calcined 300°C 5h) 100 Fe / 5 Cu / 17 Si pretreat in CO @ 280 °C 12 h & passivate in O₂ 100 Fe / 5 Cu / 4.2 K / 11 SiO₂ (calcined) 100 Fe / 5 Cu / 4.2 K / 11 SiO₂ (calcined) CO pretreat @ 280 °C 12h & passivate in O₂ for 1 h 90 Fe / 10

Mo / 5 Cu / 17 Si (calcined 300 °C 5h) 90 Fe / 10 Mo / 5 Cu / 17 Si (calcined) CO pretreat @ 280 °C + O₂ passivate 95 Fe / 5 Cr / 5 Cu / 17 Si sieved < 45 mm calcined @ 300 °C 5h * 90 Fe / 10 Cr / 5 Cu / 17 Si CO pretreat @ 280 °C 12h & passivate in O₂ for 1h 90 Fe / 10 Cr / 5 Cu / 17 Si (calcined 300 °C 5h) 90 Fe / 10 W / 5 Cu / 17 Si calcined + CO pretreat 90 Fe / 10 W / 5 Cu / 17 Si calcined @ 300 °C 5h 90 Fe / 10 W / 5 Cu / 17 Si (calcined) CO pretreat @ 280 °C 12 h + O₂ passivate 90 Fe / 10 W / 5 Cu / 17 Si prepared from WCl₆ calcined @ 300 °C 5h * 95 Fe / 5 Zr / 5 Cu / 17 Si sieved < 90 mm calcine @ 300 °C 5h * 95 Fe / 5 Mn / 5 Cu / 17 Si = 1g calcined in air @ 300 °C 5h 45-90 mm ** denotes recently synthesized (no XAS data)

CO hydrogenation reactions were carried out at 280 °C, 1.8 atm, and H₂/CO ratio = 2:1 for all catalyst samples. The catalyst sample was reduced *in situ* in flowing H₂ at 280 °C for 12 h prior to CO hydrogenation. During this quarter, we have tested the possibility that Cl impurity that may have caused the low activity of the catalyst with W addition. We prepared the catalyst with W addition using different precursors [(NH₄)₂WO₄ and WCl₆] and run CO hydrogenation reactions for the catalytic test. The activities towards CO₂ and total hydrocarbon production were shown to be similar within experimental error to the catalyst prepared from W chloride, as shown in Fig. 2. Therefore, we can definitely now conclude that the activity of the Fe-based catalyst was not promoted by the addition of W at 5 atom%.

Based on the results obtained from last quarter, we have further investigated the effect of the addition of second metals (*Me*) that result in extremely interesting high activities for CO

hydrogenation and for the water gas shift reaction. Zr, Cr and Mn are the 3 best metals able to significantly enhance the CO hydrogenation and water gas shift activity compared to the benchmark Fe catalyst. During this quarter, we have varied concentration of added Cr (3, 5, 7 and 10 atom%) in the Fe-based catalyst and studied the effect on CO hydrogenation. The formulation of catalysts studied was $(100-x)\text{Fe}/x\text{Me}/5\text{Cu}/17\text{Si}$.

The activities of Fe-based catalyst with the varying atom% of Cr for CO hydrogenation at maximum reaction rate (15 min TOS) and at the pseudo steady state of reaction (300 min TOS) are shown in Figs. 3 and 4, respectively. It is clearly seen that the CO hydrogenation activity as well as the water gas shift activity was able to be enhanced by all concentrations of added Cr compared to the benchmark Fe catalyst. Adding Cr in the range of 5 and 7 atom% appears to be the optimal concentration yielding the highest activity for CO hydrogenation (Fig. 3) and water gas shift reaction (Fig. 4). Comparisons of different %loading of Cr are shown in Fig. 5 and 6. Although adding Cr 10 atom% relative to Fe improved the catalyst activity at the beginning, the total hydrocarbon formation after 2 h declined to the same level as unpromoted Fe catalyst. The induction period of reaction was also observed for all concentrations of Cr added. It appears that adding Cr at different concentration did not perturb the behavior of the catalyst in order to form the active mixed Fe carbide as suggested in literature. This results in the same time for the catalyst to activate prior - about 15 min TOS.

The selectivity toward hydrocarbon products of the FeCr catalyst at 15 min and 300 min TOS are shown in Tables 5 and 6, respectively. The selectivity for hydrocarbon and CO_2 and $\text{C}_2\text{-C}_4$ olefins remained relatively constant within experimental error, regardless of %loading of Cr. The water gas shift activity was able to be promoted by any %loading of Cr, showing higher %selectivity to CO_2 compared to unpromoted Fe catalyst (approximately 25% enhancement). It clearly shows in Table 6 that adding Cr at any concentration had a positive impact on α compared to the benchmark Fe catalyst.

3.0 Conclusions

Characterization of catalyst showed that the BET surface area and the reduction of Fe was not significantly change by the addition of the second metals. On the other hand, the addition of Cr at any concentration in the range of 3-10 atom% to Fe FTS catalyst was able to significantly enhance the CO hydrogenation and water gas shift activity compared to the benchmark Fe catalyst. α (chain growth probability) was increased by the addition of Cr, regardless of its concentration. Adding Cr at 5 atom% appears to be the optimal concentration for CO hydrogenation and water gas shift reaction.

4.0 Next Quarter's Activities

Research carried out at Clemson University in the next quarter will be a continuation of the investigation of adding Zr and Mn to Fe-based catalyst with varying %loading. At the same time, other characterizations will be employed such as SEM and CO chemisorption for all the catalysts that have been prepared. XRD will be carried out at LSU and used to determine the phases in the as-prepared samples. Fe K_{α} excitation will be used as well as noise-free Si-based sample holders that will both greatly reduce the noise that was found from using the Rigaku Miniflex which employed Cu K_{α} excitation (which causes noise when a highly loaded Fe sample is present). Iron carbide will be synthesized to serve as a reference in the analysis of the XANES data.

